LOW ENTROPY DEEP NETWORKS

Anonymous authors
Paper under double-blind review

ABSTRACT

The movement of data between processes and memory, not arithmetic operations, dominate the energy costs of deep learning inference calculations. This work focuses on reducing these data movement costs by reducing the number of unique weights and weight-space entropy of a network. To this end, we investigate the merits of a method, which we call Weight Fixing Networks (WFN). We design the approach to realise four model outcome objectives: i) very few unique weights, ii) low-entropy weight encodings, iii) unique weight values which are amenable to energy-saving versions of hardware multiplication, and iv) lossless task-performance. Some of these goals are conflicting. To best balance these conflicts, we combine a few novel (and some well-trodden) tricks; a novel regularisation term, (i, ii) a view of clustering cost as relative distance change (i, ii, iv), and a focus on whole-network re-use of weights (i, iii). Our Imagenet experiments demonstrate lossless compression using 56x fewer unique weights and a 1.9x lower weight-space entropy than SOTA quantisation approaches.

1 INTRODUCTION

The Importance of Data Movement Costs. Although there has been a significant amount of attention exploring both algorithmic (Sze et al., 2020) and hardware-based (Chen et al., 2020) approaches to reducing the energy costs of deep learning inference, there is often a noted disconnect between the two (Sze et al., 2017). The most expensive energy costs lie in memory reads (Horowitz, 2014; Gao et al., 2017). For every off-chip DRAM data read, you pay the equivalent of over two hundred 32-bit multiplications in energy costs[1] (Horowitz, 2014). Algorithmic techniques that hope to reduce energy consumption have focussed predominantly on metrics like floating-point operations (FLOPs); intuitively, fewer FLOPs should translate into smaller energy costs from the reduced number of multiplications and potentially, fewer parameters to read from memory. However, it has been observed that this is a weak proxy for the energy consumed in running a deep learning model for inference (Sze et al., 2017). Data movement costs can still be high if we do not consider the re-use of weights, the delay between their re-use, and filter shape effects. Simply reducing the FLOPs alone does not guarantee energy cost reductions – particularly those incurred through data read and write activity.

Accelerator Design Considerations. These data movement costs are difficult to reduce in von Neumann architectures (Li et al., 2015; Sebastian et al., 2020), and so there is a move towards co-design of algorithm-hardware inference accelerators. A core consideration of accelerator design lies in exploring dataflow mappings. These mappings determine how data used in computation is distributed across memory components and optimised to take advantage of the re-use of weights, matrix multiplication partial-sums (psums), and data inputs (Han et al., 2016; Chen et al., 2017; 2015; 2020). Modern deep learning accelerators also make use of hundreds of processing elements (Chen et al., 2020) (PE's) for computation. Each PE contains a small amount of cheap and fast access memory to store a few pieces of information (weights, psums, inputs, etc.). A dataflow mapping cuts down data movement costs by making the best use of each PE and ensuring that the information they contain is recycled as much as possible. A weight/input/psum that cannot be used quickly after its latest use will be written to storage and require a re-read later. Less re-use leads to increased data movement costs. Consider, for example, weight-stationary dataflow, commonly

[1] 45nm process

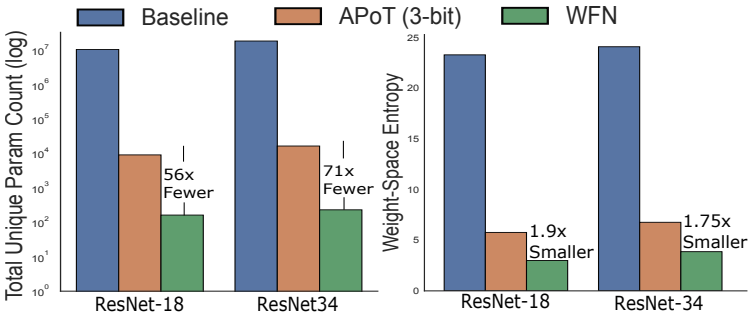

Figure 1: WFN has more weight re-use opportunities than existing quantisation approaches which can be used to reduce data movement costs. **Left**: The total number of unique parameters left after quantisation is 56x fewer than APoT for ResNet-18 trained on the Imagenet dataset and 71x for the ResNet-34 model. **Right**: The entropy of the parameters across the network is 1.9x and 1.65x smaller when using the WFN approach over APoT.

used in SOTA accelerator designs (Farshchi et al., 2019; Jouppi et al., 2017). Here the items stored statically in the PE are the model weights. Input data is then fed into the relevant PE's where multiplication is conducted locally. The ideal situation for a dataflow mapping would be to pay a single data movement cost for each unique weight value and then reference these weight values using indexing. The indexing costs can be kept low using an appropriate encoding scheme such as Huffman coding and approximated by the entropy of the weight space. Thus, the indexing access costs plus unique value access costs can be much smaller than the unquantised network (Mao & Dally, 2016; Wu et al., 2018).

Objectives. So we ask ourselves what we could do algorithmically to maximise the benefit of accelerator dataflows? We think an easy win is to reduce the number of *unique* weights a network uses. Fewer *unique* weights whilst fixing the network topology and the total number of parameters will mean that more weights are re-used more often. This additional re-use gives more opportunity to dataflows to maintain often-used weights in PE's. To further enhance the compressibility, it is desirable for the distribution of the unique weights to be concentrated around a handful of values. The high probability density weights would then be used more often and could then be reliably stored inside PE's, saving both the cost of overwriting these weight values and re-fetching them when needed later. Finally, we ask what the ideal values of these weights would be. From a computational perspective, not all multiplications are created equal. Integer powers-of-two, for example, can be implemented as simple bit-shifts. Mapping the weights used most to these values offers potential further energy reductions. Putting these three requirements together: few unique weights; a low-entropy encoding with a distribution of weights highly concentrated around a tiny subset of values; and a focus on powers-of-two values for weights — all motivated to reduce computation costs in accelerator designs — we present our contribution.

Weight Fixing Networks. Our work's overarching objective is to transform a network comprising many weights of any value (limited only by value precision) to one with the same number of weights but just a few unique values. Rather than selecting the unique weights a priori, we let the optimisation guide the process in an iterative *cluster-then-train* approach. In each iteration, we cluster an ever-increasing subset of weights to one of a few cluster centroids. We map the pre-trained network weights to these cluster centroids, which are the pool of unique weights. The training stage follows standard gradient descent optimisation to minimise performance loss with two key additions. Firstly, only an ever decreasing subset of the weights are *free* to be updated. And secondly, we use a new regularisation term to penalise weights in proportion to their nearest clusters' relative distance. We iteratively cluster subsets of weights to their nearest cluster centre, as has been demonstrated successfully previously (Zhou et al., 2017). The way we determine which subset to move is a core component of our contribution which leads to the superior compression results we achieve.

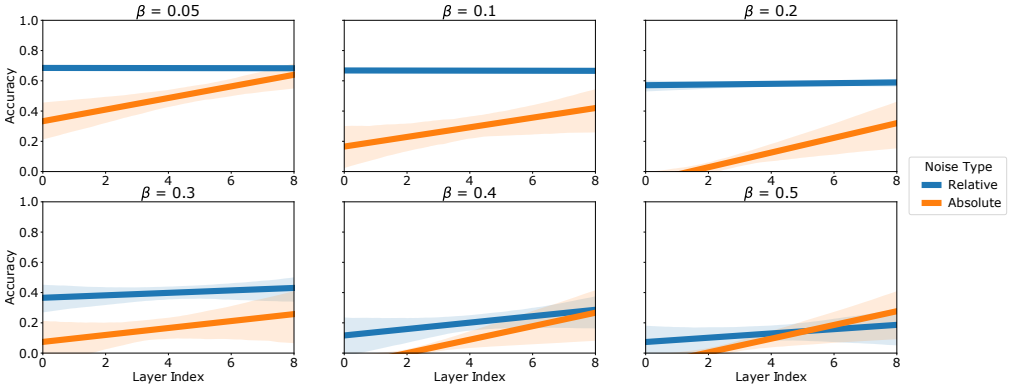

Figure 2: We explore adding relative vs absolute noise to each of the layers (x-axis). The layer index indicates which layer was selected to have noise added. Each layer index is a separate experiment with the 95% confidence intervals shaded.

Small Relative Distance Change. Rather than selecting subsets with small Euclidean distances to cluster centres, or those that have small magnitude (Zhou et al., 2017), we make the simple observation that the *relative* – as opposed to absolute – weight change matters. The distance a weight is moved when quantised is dependent on the distance between the weight w_i and its new value $w_i + \delta w_i$. When the new value is zero — as is the case for pruning methods — then the magnitude of the weight *is* the distance. Yet, this is not the case more generally. We demonstrate the importance of optimising quantisation for small relative changes with simple empirical observations. Using a pre-trained ResNet-18 model, we test adding relative vs absolute noise to the layers' weights and measure the accuracy change. For relative noise we set a noise level β and adjust all weights w_i in a layer l as: $w_i^l \leftarrow w_i^l + \mathcal{N}(0, \beta|w_i^l|)$. The standard deviation of noise added is determined by the original value w_i^l. We contrast this with absolute noise experiments, where we instead set $w_i^l \leftarrow w_i^l + \mathcal{N}(0, \beta\overline{|w^l|})$ where $\overline{|w^l|}$ corresponds to the mean absolute weight value in layer l. We run each layer-β combination experiment multiple times – to account for fluctuation in the randomised noise – and present the results in Figure 1. Even though the mean variation of noise added is the same, noise relative to the original weight value (multiplicative noise) is much better tolerated than absolute (additive noise). Since moving weights to quantisation centres is analogous to adding noise, we translate these results into our approach and prioritise weights that have small relative distances to be clustered first. We find avoiding significant quantisation errors requires ensuring that $\frac{|\delta w_i|}{|w_i|}$ is small for all weights. If this is not possible, then performance could suffer. In this case, we create an additional cluster centroid in the vicinity of an existing cluster to reduce this relative distance. Our work also challenges the almost universal trend in the literature (Yuhang Li, Xin Dong, 2020; Jung et al., 2019; Zhang et al., 2018a; Zhou et al., 2016; Yamamoto, 2021; Oh et al., 2021) of leaving the first and last layers either at full precision or 8-bit; we attempt a full network quantisation. The cost of not quantising the first layer – which typically requires the most re-use of weights due to the larger resolution of input maps – and the final linear layer – which often contains the largest number of unique weight values – is too significant to ignore.

With multiple stages of training and clustering, we finish with a significantly reduced set of unique weights. The regularisation term encourages high probability regions in the weight distribution and a lower-entropy weight-space. The initial choice of cluster centroids as powers-of-two helps us meet our third objective – energy-saving multiplication. Overall we find four distinct advantages over the works reviewed:

- We assign a cluster value to *all weights* — including the first and last layers.
- We emphasise a low entropy encoding with a regularisation term, achieving entropies smaller than even those seen using 3-bit quantisation approaches – over which we report superior performance.

- We require no additional layerwise scaling; the unique weights are shared across all layers.
- WFN substantially reduces the number of unique parameters in a network when compared to existing SOTA quantisation approaches.

2 Related Work

Clip and Scale Quantisation. Typical quantisation approaches reduce the number of bits used to represent components of the network. Quantisation has been applied to all parts of the network with varying success; the weights, gradients, and activations have all been attempted (Hubara et al., 2016; Lee et al., 2017; Jung et al., 2019; Yang et al., 2019; Shkolnik et al.; Zhou et al., 2016). Primarily, these approaches are motivated by the need to reduce the energy costs of the multiplication of 32-bit floating-point numbers. This form of quantisation uses a rounding function and scaling factor (sf) in making value adjustments where a weight w_i is mapped to a new value $w_i' = sf * round(w_i)$ for some predetermined rounding function. The scaling factor (determined by a clipping range) can be learned channel-wise (Jacob et al., 2018; Zhang et al., 2018c), or more commonly, layerwise with separate formulations. This results in different channels/layers having a diverse pool of mapping values for the network weights/activations/gradients. Quantisation can be performed without training — known as post-training quantisation, or with added training steps – called quantisation-aware training (QAT). Retraining incurs higher initial costs but results in superior performance. A clipping+scaling quantisation example relevant to our own is the work of (Zhou et al., 2017), where the authors restrict the layerwise rounding of weights to powers-of-two. The use of powers-of-two has the additional benefit of energy-cheap bit-shift multiplication. A follow-up piece of work (Yuhang Li, Xin Dong, 2020) suggests additive powers-of-two (APoT) instead to capture the pre-quantised distribution of weights better.

Weight Sharing Quantisation. Other formulations of quantisation do not use clipping and scaling factors (Stock et al., 2020; Tartaglione et al., 2021; Wu et al., 2018). Instead, they adopt clustering techniques to cluster the weights and fix the weight values to their assigned group cluster centroid. These weights are stored as codebook indices, allowing for compressed representation methods such as Huffman encoding to squeeze the network further. Unlike clipping+scaling quantisation techniques, and like ours, these methods share the pool of weights across the entire network. The work by (Wu et al., 2018) is of particular interest since both the motivation and approach are related to ours. Here the authors use a *spectrally relaxed* k-means regularisation term to encourage the network weights to be more amenable to clustering. In their case, they focus on a filter-row codebook inspired by the row-stationary dataflow used in some accelerator designs (Chen et al., 2017). However, their formulation is explored only for convolution, and they restrict clustering to groups of weights (filter rows) rather than individual weights due to computational limitations as recalibrating the k-means regularisation term is expensive during training. Similarly (Stock et al., 2020; Fan et al., 2021), focus on quantising groups of weights into single codewords rather than the individual weights themselves. Weight-sharing approaches similar to ours include (Ullrich et al., 2017). The authors use the distance from an evolving Gaussian mixture as a regularisation term to prepare the clustering weights. Although it is successful with small dataset-model combinations, the complex optimisation — particularly the additional requirement for Inverse-Gamma priors to lower-bound the mixture variance to prevent mode collapse— limits the method's practical applicability due to the high computational costs of training. In our formulation, the weights already fixed no longer contribute to the regularisation prior, reducing the computational overhead. We further reduce computation by not starting with a complete set of cluster centres but add them iteratively when needed.

3 Method

Quantisation. Consider a network $\mathcal{N}$ parameterised by N weights $W = \{w_1, ..., w_N\}$. Quantising a network is the process of reformulating $\mathcal{N}' \leftarrow \mathcal{N}$ where the new network $\mathcal{N}'$ contains weights which all take values from a reduced pool of k cluster centres $C = \{c_1, ..., c_k\}$ where $k \ll N$. After quantisation, each of the connection weights in the original network is replaced by one of the cluster centres $w_i \leftarrow c_j$, $W' = \{w_i' | w_i' \in C, i = 1, \cdots, N\}$, $|W'| = k$, where W' is the set of

weights of the new network $\mathcal{N}'$, which has the same topology as the original $\mathcal{N}$.

Method Outline. WFN is comprised of T *fixing iterations* where each iteration $t \in T$ has a training and a clustering stage. The clustering stage is tasked with partitioning the weights into two subsets $W = W^t_{fixed} \cup W^t_{free}$. W^t_{fixed} is the set of weights fixed at one of the cluster centre values $c_k \in C$. The weights $w_i \in W^t_fixed$ are not updated by gradient decent in this, nor any subsequent training stages, these weights are *fixed*. In contrast, the *free-weights* denoted by W^t_{free} remain trainable during the next training stage. With each subsequent iteration t we increase the proportion of weights that take on fixed cluster centre values p_t such that $p_0 < p_1 \ldots < p_T$, where $p_t = \frac{|W^t_{fixed}|}{|W|}$. By iteration T, all weights will be fixed to one of the cluster centres making $p_T = 1$. The training stage combines gradient descent based error correction along with a tight-cluster regularisation term and is tasked with maintaining lossless performance as we fix more of the weights to cluster centres.

Clustering Stage. In the clustering stage, we work backwards from our goal of minimising the relative distance travelled for each of the weights to determine which values cluster centres $c_i \in C$ should take. Given a weight $w_i \in W$ and cluster centre $c_j \in C$ we use a distance function $D(w_i, c_j) = |w_i - c_j|$ and the original weight value w_i to define a relative distance measure $D_{rel}(w_i, c_j) = \frac{D(w_i, c_j)}{|w_i|}$. Normalising by w_i ensures that distance is measured proportionally to the original weight value, rather than in absolute terms. To use this in determining the cluster centres, we enforce a threshold δ on this relative distance, $D_{rel}(w_i, c_j) \leq \delta$ for small δ. We can then define the cluster centres $c_j \in C$ which make this possible using a simple recurrence relation. Assume we have a starting cluster centre value c_j, we want the neighbouring cluster value c_{j+1} to be such that if a network weight w_i is between these clusters $w_i \in [c_j, \frac{c_{j+1}+c_j}{2}]$ then $D_{rel}(w_i, c_j) \leq \delta$. Plugging in $\frac{c_{j+1}+c_j}{2}$ and c_j into D_{rel} and setting it equal to δ we have:

$$\frac{|\frac{c_{j+1}+c_j}{2} - c_j|}{\frac{c_{j+1}+c_j}{2}} = \delta, \tag{1}$$

this leads to a recurrence relation:

$$c_{j+1} = c_j(\frac{1+\delta}{1-\delta}),\ 0 < \delta < 1, \tag{2}$$

that provides the next cluster centre value given the previous one. With this, we can generate all the cluster centres given some boundary conditions. Starting with some value c_0, we generate c_1 which is then used to generate c_2 and so on. We introduce the lower-bound cluster threshold $c_0 = \delta_0$, which we use to generate the cluster centres and any absolute weight value that is less than δ_0 is assigned the cluster value 0. This lower bound serves two purposes: firstly, it reduces the number of proposal cluster centres which would otherwise increase exponentially in density around zero, and additionally, the zero-valued weights will allow sparsity-leveraging hardware to avoid operations that use these weights, reducing the computational overhead. As an upper-bound, we stop the recurrence once a cluster centre is larger than the maximum weight in the network, $\max_j |c_j| \leq \max_i |w_i|,\ w_i \in W, c_j \in C$.

Generating the Proposed Cluster centres. Putting this together, we have a starting point $c_0 = \delta_0$, a recurrence relation to produce cluster centres given c_0 that maintains a relative distance change when weights are moved to their nearest cluster centre, and a centre generation stopping condition $c_j \leq \max_{i \in W} |w_i|, c_j \in C$. We use the δ_0 value as our first proposed cluster centre c_0 with the recurrence relation generating a proposed cluster set of size s. Since all these values will contain only positive values, we join this set with its negated version along with a zero value to create a proposal cluster set $C^S = \{a(\frac{1+\delta}{1-\delta})^j \delta_0 \mid j = 0, 1 \cdots s;\ a = +1, 0, -1\}$ of size $2s + 1$.

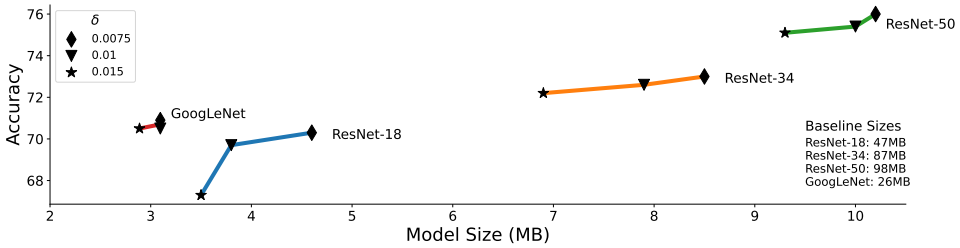

Figure 3: The accuracy vs model size trade-off can be controlled by the δ parameter. All experiments shown are using the ImageNet dataset, accuracy refers to top-1.

To account for the zero threshold δ_0 and for ease of notation as we advance, we make a slight amendment to the definition of the relative distance function $D_{rel}(w_i, c_j)$:

$$D^{+}_{rel}(w_i, c_j) = \begin{cases} \frac{D(w_i, c_j)}{|w_i|}, & \text{if } |w_i| \geq \delta_0 \\ 0, & \text{otherwise} \end{cases} \tag{3}$$

Reducing k with Additive Powers-of-two Approximations. Although using all of the values in C^S as centres to cluster the network weights would meet the requirement for the relative movement of weights to their closest cluster to be less than δ, it would also require a large number of $k = |C^S|$ clusters. In addition, the values in C^S are also of full 16-bit precision, and we would prefer many of the weights to be powers-of-two for ease of multiplication in hardware. With the motivation of reducing k and encouraging powers-of-two clusters whilst maintaining the relative distance movement where possible, we look to a many-to-one mapping of the values of C^S to further cluster the cluster centres. Building on the work of others (Zhou et al., 2017; Yuhang Li, Xin Dong, 2020), we map each of the values $c_i \in C^S$ to their nearest power-of-two, $round(c_i) = sgn(c_i)2^{\lfloor log_2(c_i) \rceil}$ and, for flexibility, we further allow for *additive* powers-of-two rounding. With additive powers-of-two rounding, each cluster value can also come from the sum of powers-of-two values (b-bit) up to order ω where the order represents the number of powers-of-two that can contribute to the approximation[2]. As an example, given $c_k = 0.45, c_k \in C^S$, an $\omega = 1$ approximation would round c_k to its nearest power-of-two $c^1_k = \frac{1}{2^1} = 0.5$ whereas an order $\omega = 2$ approximation is $c^2_k = \frac{1}{2^1} - \frac{1}{2^4} = 0.4375$. A higher-order grants a better approximation, but at the cost of more cluster centroids overall and requires ω bit-shifts + additions in hardware. We give full details of the algorithm to map the proposal set C^S to the ω-order approximation $\widetilde{C}^{\omega}$ in the Appendix.

Minimalist Clustering. We are now ready to present the clustering procedure for a particular iteration t, which we give the pseudo-code for in Algorithm 1. We start the iteration with $\omega = 1$ and a set of weights not yet fixed W^t_{free}. For the set of cluster centres $\widetilde{C}^{\omega}$ of order ω, let $c^{\omega}_*(i) = \min_{c \in \widetilde{C}^{\omega}} D^{+}_{\text{rel}}(w_i, c)$ be the one closest to weight w_i. $n^{\omega}_k = \sum_i \mathbb{I}[c^{\omega}_k = c^{\omega}_*(i)]$ counts the number of weights assigned to cluster centre $c^{\omega}_k \in \widetilde{C}^{\omega}$, where the indicator function $\mathbb{I}[x]$ is 1 if x is true and 0 otherwise. Let $k^* = \arg\max_k n^{\omega}_k$ so that $c^{\omega}_{k^*}$ is the modal cluster. For the cluster k^* let permutation π of $\{1, \ldots, N\}$ that maps $w_i \mapsto w'_{\pi(i)}$, be such that the sequence $(w'_1(k^*), w'_2(k^*), \ldots, w'_N(k^*))$ is arranged in ascending order of relative distance from the cluster $c^{\omega}_{k^*}$. In other words, $D^{+}_{\text{rel}}(w'_i(k^*), c^{\omega}_{k^*}) \leq D^{+}_{\text{rel}}(w'_{i+1}(k^*), c^{\omega}_{k^*})$, for $i = 1, \ldots, (N-1)$. We choose n to be the largest integer such that:

$$\sum_{i=1}^{n} D^{+}_{\text{rel}}(w'_i(k^*), c^{\omega}_{k^*}) \leq n\delta, \text{ and } \sum_{i=1}^{n+1} D^{+}_{\text{rel}}(w'_i(k^*), c^{\omega}_{k^*}) > (n+1)\delta, \tag{4}$$

[2]The notion of an order has been identified recently in work parallel to ours (Oh et al., 2021), where the term *word* is used instead, i.e. *two-word* directly translates into an $\omega = 2$.

and define $\{w'_1, w'_2, \ldots, w'_n\}$ to be the set of weights to be fixed at this stage of the iteration. These are the weights that can be moved to the cluster centre $c^{\omega}_{k^*}$ without exceeding the average relative distance δ of the weights from the centre. The corresponding weight indices from the original network $\mathcal{N}$ are in $\{\pi^{-1}(1), \ldots, \pi^{-1}(n)\}$, and called $fixed_{new}$in the algorithm. If there are no such weights that can be found, *i.e.*, for some cluster centre l^*, the minimum relative distance $D^{+}_{\text{rel}}(w'_1(l^*), c_{l^*}) > \delta$, the corresponding set $fixed_{new}$ is empty. In this case, there are no weights that can move to this cluster centre without breaking the δ constraint and we increase order $\omega \leftarrow \omega + 1$ to compute a new $c^{\omega}_{k^*}$, repeating the process until $|fixed_{new}| > 0$. Once the condition $|fixed_{new}| > 0$ is satisfied, we fix the identified weights $\{w'_1, w'_2, \ldots, w'_n\}$ to their corresponding cluster centre value $c^{\omega}_{k^*}$ and move them into W^{t+1}_{fixed}. We continue the process of identifying cluster centres and fixing weights to these centres until $|W^{t+1}_{fix}| \geq Np_t$, at which point the iteration t is complete and the training stage of iteration $t + 1$ begins. Our experiments found that a larger δ has less impact on task performance during early t iterations and so we reduce δ linearly with each increasing $t \in T$ (full details in the Appendix). We will show later that, with a small δ, over 75% of the weights can be fixed with $\omega = 1$ and over 95% of weights with $\omega \leq 2$.

Training Stage. Despite the steps taken to minimise the impact of the clustering stage, without retraining, performance would suffer. To negate this, we perform gradient descent to adjust the remaining free weights W^t_{free}. This allows the weights to correct for any loss increase incurred after clustering where training aims to select values W^t_{free} that minimise the usual loss (cross-entropy in our case) whilst W_{fixed} remain unchanged.

Cosying up to Clusters. Having the remaining W^t_{free} weights closer to the cluster centroids C post-training makes clustering less damaging to performance. We coerce this situation by adding a regularisation term — given in Equation 5 — to the retraining where $p(c_j|w_i) = \frac{e^{-D^{+}_{reg}(w_i, c_j)}}{\sum^k_l e^{-D^{+}_{reg}(w_i, c_l)}}$. The idea is to penalise the free-weights W^t_{free} proportionally to their distance away from the clusters to which they are most likely to be assigned — i.e. the closest. Clusters that are unlikely to be weight w_i's nearest — and therefore final fixed value — do not contribute much to the penalisation term. We balance this regularisation term against the cross-entropy training loss with the γ hyper-parameter, which we fix to be a α proportion of the other loss term $\gamma = \alpha \frac{\mathcal{L}_{cross_entropy}}{\mathcal{L}_{reg}}$. We note that the γ term is detached from the computational graph and treated as a constant (otherwise the L_{reg} term would cancel).

$$\mathcal{L}_{reg} = \gamma \sum_{i \in W_{free}}^{N} \sum_{j}^{k} D^{+}_{reg}(w_i, c_j) p(c_j|w_i) \tag{5}$$

4 Experiment Details

We apply WFN to fully converged models trained on the CIFAR-10 and ImageNet datasets. Our pre-trained models are all publicly available with strong baseline accuracies[3]: Resnet-(18,34,50) (Wu et al., 2017), MobileNetV2 (Sandler et al., 2018) and, GoogLeNet (Chollet, 2017). We run ten weight-fixing iterations for three epochs, increasing the percentage of weights fixed until all weights are fixed to a cluster. In total, we train for 30 epochs per experiment using the Adam optimiser (Kingma & Ba, 2015) with a learning rate 2×10^{-5}. We use grid-search to explore hyper-parameter combinations using ResNet-18 and MobileNetV2 models with the CIFAR-10 dataset and find that the regularisation weighting $\alpha = 0.4$ works well across all experiments reducing the need to further hyper-parameter tuning as we advance. The distance threshold δ gives the practitioner control over the compression-performance trade-off (see Figure 3), and so we report a range of values. We give full details of the experiments run along with the results of a hyper-parameter ablation study using CIFAR-10 in the Appendix.

[3]CIFAR-10 models : https://github.com/kuangliu/pytorch-cifar, ImageNet models: torchvision

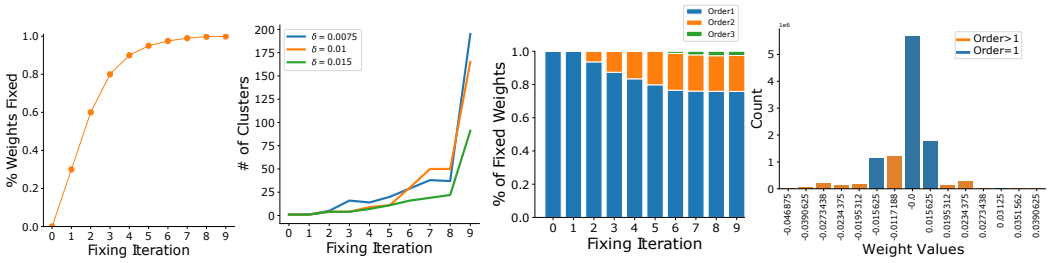

Figure 4: **Far left:** We increase the number of weights in the network that are fixed to cluster centres with each fixing iteration. **Middle left:** Here, we show how decreasing the δ threshold increases the number of cluster centres, but only towards the last few fixing iterations, which helps keep the weight-space entropy down. **Middle right:** The majority of all weights are order 1 (powers-of-two), the increase in order is only needed for outlier weights in the final few fixing iterations. **Far right:** The weight distribution (top-15 most used show) is concentrated around just four values. All of these charts are produced with ResNet-18 models trained on the ImageNet dataset.

5 RESULTS

		Accuracy (%)					Accuracy (%)		
Model	**Method**	**Top-1**	**Top-5**	**CR**	**Model**	**Method**	**Top-1**	**Top-5**	**CR**
ResNet-18	Baseline	68.9	88.9	1.0	ResNet-34	Baseline	73.3	90.9	1.0
	LQ-Net	68.2	87.9	7.7		LQ-Net	71.9	90.2	8.6
	APoT	69.9	89.2	10.2		APoT	73.4	91.1	10.6
	LSQ	70.2^{+}	89.4^{+}	9.0*		LSQ	73.4^{+}	91.4^{+}	9.2*
	WFN ($\delta = 0.015$)	67.3	87.6	13.4		WFN($\delta = 0.015$)	72.2	90.9	12.6
	WFN ($\delta = 0.01$)	69.7	89.2	12.3		WFN ($\delta = 0.01$)	72.6	91.0	11.1
	WFN ($\delta = 0.0075$)	70.3	89.1	10.2		WFN ($\delta = 0.0075$)	73.0	91.2	10.3
ResNet-50	Baseline	76.1	92.8	1.0	GoogLeNet	Baseline	69.7	89.6	1.0
	LQ-Net	74.2	91.6	5.9		Deep k-Means	69.4	89.7	3.0
	APoT	75.8	92.7	9.0		GreBdec	67.3	88.9	4.5
	LSQ	75.8^{+}	92.7^{+}	8.1*		KQ	69.2	-	5.8
	WFN ($\delta = 0.015$)	75.1	92.1	10.3		WFN($\delta = 0.015$)	70.5	89.9	9.0
	WFN ($\delta = 0.01$)	75.4	92.5	9.8		WFN ($\delta = 0.01$)	70.5	90.0	8.4
	WFN ($\delta = 0.0075$)	76.0	92.7	9.5		WFN ($\delta = 0.0075$)	70.9	90.2	8.4

Table 1: A comparison of WFN against other quantisation and weight clustering approaches. The WFN pipeline is able to achieve higher compression ratios than the works compared whilst matching or improving upon baseline accuracies.

* Estimated from the LSQ paper model size comparison graph, we over-estimate to be as fair as possible.
$^{+}$ Open-source implementations have so far been unable to replicated the reported results: https://github.com/hustzxd/LSQuantization.

5.1 RESULTS

We begin by comparing WFN for a range of δ values against a diverse set of quantisation approaches that have comparable compression ratios (CR) in Table 5. The 3-bit quantisation methods we compare include: LSQ (Esser et al., 2020), LQ-Net (Zhang et al., 2018b) and APoT (Yuhang Li, Xin Dong, 2020). We additionally compare with the clustering-quantisation methods using the GoogLeNet model: Deep-k-Means (Wu et al., 2018) whose method is similar to ours, KQ (Yu et al., 2020), and GreBdec (Yu et al., 2017). Whilst the results demonstrate WFN's lossless performance with SOTA CR, this is not the main motivation for the method. Instead, we are interested in how WFN can reduce the number of unique parameters in a network and corresponding weight-space entropy which together give the potential benefit of future accelerator designs to reduce data movement costs. We note to the interested reader there are additional theoretical reasons for pursuing low weight-space entropy networks (Hinton & van Camp, 1993; Grünwald, 2000; Hansen & Yu, 2001), but our primary focus is from the perspective of reducing accelerator data movement costs.

Capturing the benefit of algorithmic developments to reduce data movement costs in accelerator designs is non-trivial due to the significant dependency on architecture memory hierarchy, communication orchestration costs and the dataflow mapping used. Some active works attempt to provide robust estimations in bridging the gap between estimation and actual energy costs, through acceler-

Model	Method	Top-1	Entropy	Param Count	$Rep'(\mathcal{N}')$	Model Size
ResNet-18	Baseline	68.9	23.3	10756029	1.000	46.8MB
	APoT (3bit)	69.9	5.77	9237	0.283	4.56MB
	WFN ($\delta = 0.015$)	67.3	2.72	90	0.005	3.5MB
	WFN ($\delta = 0.01$)	69.7	3.01	164	0.007	3.8MB
	WFN ($\delta = 0.0075$)	70.3	4.15	193	0.018	4.6MB
ResNet-34	Baseline	73.3	24.1	19014310	1.000	87.4MB
	APoT (3bit)	73.4	6.77	16748	0.296	8.23MB
	WFN ($\delta = 0.015$)	72.2	2.83	117	0.002	6.9MB
	WFN ($\delta = 0.01$)	72.6	3.48	164	0.002	7.9MB
	WFN ($\delta = 0.0075$)	73.0	3.87	233	0.004	8.5MB
ResNet-50	Baseline	76.1	24.2	19915744	1.000	97.5MB
	WFN ($\delta = 0.015$)	75.1	3.55	125	0.002	9.3MB
	WFN ($\delta = 0.01$)	75.4	4.00	199	0.002	10.0MB
	WFN ($\delta = 0.0075$)	76.0	4.11	261	0.003	10.2MB

Table 2: A full metric comparison of WFN Vs. APoT.

ator mapping estimation (Kwon et al., 2019) or fixing the mapping and estimating the energy costs on a particular accelerator (Yang et al., 2017). However, support is limited to specific fixed architecture designs and does not account for the referenced weight-sharing. Instead, we rely on analytical metrics as a proxy such as the one proposed by (Wu et al., 2018) itself a subset of measurements conducted by (Sakr et al., 2017) (Equation 6) which attempts to estimate the weight representation (and correlated data movement) energy costs as the product of N_w, B_w and $|W|$, which refer to the number of operations the weights are involved in, the weight-representation bit-width for each weight, and the unique weights in the network, respectively. Due to the low weight-space entropy we achieve, we suggest Huffman encoding to represent the network index-set (as is used by various accelerator designs (Moons & Verhelst, 2016; Han et al., 2016)) and so the weight-representational bit-width will vary for each weight. We amend the original formulation to account for this (Eq 7). Here N_{w_i} is the number of times weight w_i is used in during an inference computation, and B_{w_i} refers to the Huffman-encoded representation bit-width of w_i.

$$Rep(\mathcal{N}') = N_w|W|B_w \tag{6}$$

$$Rep'(\mathcal{N}') = \sum_{w_i \in W} N_{w_i} B_{w_i} \tag{7}$$

The authors of the APoT have released the quantised model weights and code, and we use the released model-saves[4] of this SOTA model to compare the entropy, $Rep'(\mathcal{N}')$, unique parameter count, model size and accuracy in Table 2. Our work outperforms APoT in weight-space entropy, unique parameter count and weight representational cost by a large margin. Taking the ResNet-18 experiments as an example, the reduction to just 164 weights compared with APoT's 9237 demonstrates the effectiveness of WFN. This is in part due to our full-network quantisation (APoT, as aforementioned, does not quantise the first, last and batch-norm parameters), but even when we discount these advantages and look at weight subsets ignoring the first, last and batch-norm layers WFN uses many times fewer parameters and half the weight-space entropy. We provide a further breakdown of these results in the Appendix. Finally, let us examine how WFN achieves the substantial reduction in weight-space entropy. In Figure 4 we see that not only do the resultant WFN networks have very few unique weights, but the weight distribution is such that the vast majority of all of the weights are a small handful of powers-of-two values (order 1) and the other unique weights (outside of the top 4) are of low frequency and added only in the final fixing iterations.

6 Conclusion

We have presented WFN, a compression pipeline that can successfully compress whole neural networks. A single network codebook, focusing on reducing entropy of the weight-space coupled with the number of unique weights in the network. The WFN process produces highly compressible and hardware-friendly representations of networks using just a few unique weights without performance degradation. Although the results demonstrate strong compression ability, few unique parameters, and low weight-space entropy, the true potential of the method is that it will gives accelerator designers more scope for weight re-use, keeping most/all weights close to computation,

[4]https://github.com/yhhhli/APoT_Quantization

reducing the energy-hungry data movement costs.

REFERENCES

Yiran Chen, Yuan Xie, Linghao Song, Fan Chen, and Tianqi Tang. A Survey of Accelerator Architectures for Deep Neural Networks. *Engineering*, 6(3):264–274, 2020. ISSN 20958099. doi: 10.1016/j.eng.2020.01.007. URL https://doi.org/10.1016/j.eng.2020.01.007.

Yu Hsin Chen, Tushar Krishna, Joel S. Emer, and Vivienne Sze. Eyeriss: An Energy-Efficient Reconfigurable Accelerator for Deep Convolutional Neural Networks. *IEEE J. Solid-State Circuits*, 52(1):127–138, jan 2017. ISSN 00189200. doi: 10.1109/JSSC.2016.2616357.

Yunji Chen, Tao Luo, Shaoli Liu, Shijin Zhang, Liqiang He, Jia Wang, Ling Li, Tianshi Chen, Zhiwei Xu, Ninghui Sun, and Olivier Temam. DaDianNao: A Machine-Learning Supercomputer. In *Proc. Annu. Int. Symp. Microarchitecture, MICRO*, 2015. ISBN 9781479969982. doi: 10.1109/MICRO.2014.58.

François Chollet. Xception: Deep learning with depthwise separable convolutions. In *Proc. - 30th IEEE Conf. Comput. Vis. Pattern Recognition, CVPR 2017*, 2017. ISBN 9781538604571. doi: 10.1109/CVPR.2017.195.

Steven K Esser, Jeffrey L. McKinstry, Deepika Bablani, Rathinakumar Appuswamy, and Dharmendra S Modha. Learned Step Size Quantization. *8th Int. Conf. Learn. Represent. ICLR 2020*, 2020. URL http://arxiv.org/abs/1902.08153.

Angela Fan, Pierre Stock, Benjamin Graham, Edouard Grave, Remi Gribonval, Herve Jegou, and Armand Joulin. Training with Quantization Noise for Extreme Model Compression. *9th Int. Conf. Learn. Represent. ICLR 2021 - Conf. Track Proc.*, apr 2021. URL http://arxiv.org/abs/2004.07320.

Farzad Farshchi, Qijing Huang, and Heechul Yun. Integrating NVIDIA Deep Learning Accelerator (NVDLA) with RISC-V SoC on FireSim. In *Proc. - 2019 2nd Work. Energy Effic. Mach. Learn. Cogn. Comput. Embed. Appl. EMC2 2019*, 2019. ISBN 9781728167633. doi: 10.1109/EMC249363.2019.00012.

Mingyu Gao, Jing Pu, Xuan Yang, Mark Horowitz, and Christos Kozyrakis. TETRIS: Scalable and efficient neural network acceleration with 3D memory. *ACM SIGPLAN Not.*, 2017. ISSN 15232867. doi: 10.1145/3037697.3037702.

P. Grünwald. Model selection based on minimum description length. *J. Math. Psychol.*, 44(1): 133–152, mar 2000. ISSN 00222496. doi: 10.1006/jmps.1999.1280.

Song Han, Xingyu Liu, Huizi Mao, Jing Pu, Ardavan Pedram, Mark A. Horowitz, and William J. Dally. EIE: Efficient Inference Engine on Compressed Deep Neural Network. feb 2016. URL http://arxiv.org/abs/1602.01528.

Mark H. Hansen and Bin Yu. Model selection and the principle of minimum description length. *J. Am. Stat. Assoc.*, 96(454):746–774, 2001. ISSN 1537274X. doi: 10.1198/016214501753168398. URL https://www.jstor.org/stable/2670311.

Geoffrey E Hinton and Drew van Camp. Keeping neural networks simple by minimizing the description length of the weights. pp. 5–13, 1993. ISBN 0897916115. doi: 10.1145/168304.168306.

Mark Horowitz. 1.1 Computing's energy problem (and what we can do about it). In *Dig. Tech. Pap. - IEEE Int. Solid-State Circuits Conf.*, 2014. ISBN 9781479909186. doi: 10.1109/ISSCC.2014.6757323.

Itay Hubara, Matthieu Courbariaux, Daniel Soudry, Ran El-Yaniv, and Yoshua Bengio. Binarized neural networks. In *Adv. Neural Inf. Process. Syst.*, 2016.

Benoit Jacob, Skirmantas Kligys, Bo Chen, Menglong Zhu, Matthew Tang, Andrew Howard, Hartwig Adam, and Dmitry Kalenichenko. Quantization and Training of Neural Networks for Efficient Integer-Arithmetic-Only Inference. In *Proc. IEEE Comput. Soc. Conf. Comput. Vis. Pattern Recognit.*, pp. 2704–2713, 2018. ISBN 9781538664209. doi: 10.1109/CVPR.2018.00286.

Norman P. Jouppi, Cliff Young, Nishant Patil, David Patterson, Gaurav Agrawal, Raminder Bajwa, Sarah Bates, Suresh Bhatia, Nan Boden, Al Borchers, Rick Boyle, Pierre Luc Cantin, Clifford Chao, Chris Clark, Jeremy Coriell, Mike Daley, Matt Dau, Jeffrey Dean, Ben Gelb, Tara Vazir Ghaemmaghami, Rajendra Gottipati, William Gulland, Robert Hagmann, C. Richard Ho, Doug Hogberg, John Hu, Robert Hundt, Dan Hurt, Julian Ibarz, Aaron Jaffey, Alek Jaworski, Alexander Kaplan, Harshit Khaitan, Daniel Killebrew, Andy Koch, Naveen Kumar, Steve Lacy, James Laudon, James Law, Diemthu Le, Chris Leary, Zhuyuan Liu, Kyle Lucke, Alan Lundin, Gordon MacKean, Adriana Maggiore, Maire Mahony, Kieran Miller, Rahul Nagarajan, Ravi Narayanaswami, Ray Ni, Kathy Nix, Thomas Norrie, Mark Omernick, Narayana Penukonda, Andy Phelps, Jonathan Ross, Matt Ross, Amir Salek, Emad Samadiani, Chris Severn, Gregory Sizikov, Matthew Snelham, Jed Souter, Dan Steinberg, Andy Swing, Mercedes Tan, Gregory Thorson, Bo Tian, Horia Toma, Erick Tuttle, Vijay Vasudevan, Richard Walter, Walter Wang, Eric Wilcox, and Doe Hyun Yoon. In-datacenter performance analysis of a tensor processing unit. In *Proc. - Int. Symp. Comput. Archit.*, 2017. ISBN 9781450348928. doi: 10.1145/3079856.3080246.

Sangil Jung, Changyong Son, Seohyung Lee, Jinwoo Son, Jae Joon Han, Youngjun Kwak, Sung Ju Hwang, and Changkyu Choi. Learning to quantize deep networks by optimizing quantization intervals with task loss. In *Proc. IEEE Comput. Soc. Conf. Comput. Vis. Pattern Recognit.*, 2019. ISBN 9781728132938. doi: 10.1109/CVPR.2019.00448.

Diederik P. Kingma and Jimmy Lei Ba. Adam: A method for stochastic optimization. In *3rd Int. Conf. Learn. Represent. ICLR 2015 - Conf. Track Proc.*, 2015.

Hyoukjun Kwon, Prasanth Chatarasi, Michael Pellauer, Angshuman Parashar, Vivek Sarkar, and Tushar Krishna. Understanding reuse, performance, and hardware cost of DNN dataflows: A data-centric approach. In *Proc. Annu. Int. Symp. Microarchitecture, MICRO*, 2019. ISBN 9781450369381. doi: 10.1145/3352460.3358252.

Edward H. Lee, Daisuke Miyashita, Elaina Chai, Boris Murmann, and S. Simon Wong. LogNet: Energy-efficient neural networks using logarithmic computation. In *ICASSP, IEEE Int. Conf. Acoust. Speech Signal Process. - Proc.*, 2017. ISBN 9781509041176. doi: 10.1109/ICASSP.2017.7953288.

H. Li, B. Gao, Z. Chen, Y. Zhao, P. Huang, H. Ye, L. Liu, X. Liu, and J. Kang. A learnable parallel processing architecture towards unity of memory and computing. *Sci. Rep.*, 2015. ISSN 20452322. doi: 10.1038/srep13330.

Huizi Mao and William J Dally. Deep Compression: Compressing Deep Neural. *Iclr 2016*, pp. 1–14, 2016. URL `https://arxiv.org/abs/1510.00149`.

Bert Moons and Marian Verhelst. A 0.3-2.6 TOPS/W precision-scalable processor for real-time large-scale ConvNets. *IEEE Symp. VLSI Circuits, Dig. Tech. Pap.*, 2016-Septe:1–2, 2016. doi: 10.1109/VLSIC.2016.7573525.

Sangyun Oh, Hyeonuk Sim, Sugil Lee, and Jongeun Lee. Automated Log-Scale Quantization for Low-Cost Deep Neural Networks. *Proc. IEEE/CVF Conf. Comput. Vis. Pattern Recognit.*, 2021.

Charbel Sakr, Yongjune Kim, and Naresh Shanbhag. Analytical guarantees on numerical precision of deep neural networks. *34th Int. Conf. Mach. Learn. ICML 2017*, 6:4603–4615, 2017.

Mark Sandler, Andrew Howard, Menglong Zhu, Andrey Zhmoginov, and Liang Chieh Chen. MobileNetV2: Inverted Residuals and Linear Bottlenecks. *Proc. IEEE Comput. Soc. Conf. Comput. Vis. Pattern Recognit.*, pp. 4510–4520, 2018. ISSN 10636919. doi: 10.1109/CVPR.2018.00474.

Abu Sebastian, Manuel Le Gallo, Riduan Khaddam-Aljameh, and Evangelos Eleftheriou. Memory devices and applications for in-memory computing, 2020. ISSN 17483395.

Moran Shkolnik, Brian Chmiel, Ron Banner, Gil Shomron, Yury Nahshan, Alex Bronstein, and Uri Weiser. Robust Quantization: One Model to Rule Them All. Technical report.

Pierre Stock, Armand Joulin, Rémi Gribonval, Benjamin Graham, and Hervé Jégou. And the bit goes down: Revisiting the quantization of neural networks, 2020. ISSN 23318422.

Vivienne Sze, Yu-Hsin Chen, Tien-Ju Yang, and Joel Emer. Efficient Processing of Deep Neural Networks: A Tutorial and Survey. mar 2017. URL http://arxiv.org/abs/1703.09039.

Vivienne Sze, Yu-Hsin Chen, Tien-Ju Yang, and Joel S. Emer. Efficient Processing of Deep Neural Networks. *Synth. Lect. Comput. Archit.*, 2020. ISSN 1935-3235. doi: 10.2200/s01004ed1v01y202004cac050.

Enzo Tartaglione, Stéphane Lathuilière, Attilio Fiandrotti, Marco Cagnazzo, and Marco Grangetto. HEMP: High-order Entropy Minimization for neural network comPression. 2021. doi: 10.1016/j.neucom.2021.07.022. URL http://arxiv.org/abs/2107.05298{%}0Ahttp://dx.doi.org/10.1016/j.neucom.2021.07.022.

Karen Ullrich, Edward Meeds, and Max Welling. Soft weight-sharing for neural network compression. *arXiv*, pp. 1–16, 2017.

Junru Wu, Yue Wang, Zhenyu Wu, Zhangyang Wang, Ashok Veeraraghavan, and Yingyan Lin. Deep κ-means: Re-training and parameter sharing with harder cluster assignments for compressing deep convolutions. *35th Int. Conf. Mach. Learn. ICML 2018*, 12:8523–8532, 2018.

Songtao Wu, Shenghua Zhong, and Yan Liu. ResNet. *Multimed. Tools Appl.*, 2017. ISSN 15737721. doi: 10.1007/s11042-017-4440-4.

Kohei Yamamoto. Learnable Companding Quantization for Accurate Low-bit Neural Networks. pp. 5029–5038, 2021. URL http://arxiv.org/abs/2103.07156.

Jiwei Yang, Xu Shen, Jun Xing, Xinmei Tian, Houqiang Li, Bing Deng, Jianqiang Huang, and Xian Sheng Hua. Quantization networks. In *Proc. IEEE Comput. Soc. Conf. Comput. Vis. Pattern Recognit.*, 2019. ISBN 9781728132938. doi: 10.1109/CVPR.2019.00748.

Tien Ju Yang, Yu Hsin Chen, and Vivienne Sze. Designing energy-efficient convolutional neural networks using energy-aware pruning. In *Proc. - 30th IEEE Conf. Comput. Vis. Pattern Recognition, CVPR 2017*, 2017. ISBN 9781538604571. doi: 10.1109/CVPR.2017.643.

Xiyu Yu, Tongliang Liu, Xinchao Wang, and Dacheng Tao. On compressing deep models by low rank and sparse decomposition. *Proc. - 30th IEEE Conf. Comput. Vis. Pattern Recognition, CVPR 2017*, 2017-Janua:67–76, 2017. doi: 10.1109/CVPR.2017.15.

Zhongzhi Yu, Yemin Shi, Tiejun Huang, and Yizhou Yu. Kernel Quantization for Efficient Network Compression. 2020. URL http://arxiv.org/abs/2003.05148.

Wei Wang Yuhang Li, Xin Dong. Additive Powers-of-Two Quantization: an Efficient Non-Uniform Discretization for Neural Networks. *Iclr*, (2014):2016–2019, 2020. URL https://openreview.net/pdf?id=BkgXT24tDS.

Dongqing Zhang, Jiaolong Yang, Dongqiangzi Ye, and Gang Hua. LQ-Nets: Learned quantization for highly accurate and compact deep neural networks. In *Lect. Notes Comput. Sci. (including Subser. Lect. Notes Artif. Intell. Lect. Notes Bioinformatics)*, volume 11212 LNCS, pp. 373–390, 2018a. ISBN 9783030012366. doi: 10.1007/978-3-030-01237-3_23. URL https://github.com/Microsoft/LQ-Nets.

Dongqing Zhang, Jiaolong Yang, Dongqiangzi Ye, and Gang Hua. LQ-Nets: Learned quantization for highly accurate and compact deep neural networks. In *Lect. Notes Comput. Sci. (including Subser. Lect. Notes Artif. Intell. Lect. Notes Bioinformatics)*, 2018b. ISBN 9783030012366. doi: 10.1007/978-3-030-01237-3_23.

Dongqing Zhang, Jiaolong Yang, Dongqiangzi Ye, and Gang Hua. LQ-Nets: Learned quantization for highly accurate and compact deep neural networks, 2018c. ISSN 23318422. URL https://github.com/Microsoft/LQ-Nets.

Aojun Zhou, Anbang Yao, Yiwen Guo, Lin Xu, and Yurong Chen. Incremental network quantization: Towards lossless cnns with low-precision weights, 2017.

Shuchang Zhou, Yuxin Wu, Zekun Ni, Xinyu Zhou, He Wen, and Yuheng Zou. DoReFa-Net: Training Low Bitwidth Convolutional Neural Networks with Low Bitwidth Gradients. jun 2016. URL http://arxiv.org/abs/1606.06160.

A APPENDIX

A.1 THE WFN OVERVIEW ALGORITHM

Algorithm 1: Clustering Np_t weights at the tth iteration.

while $|W_{fix}^{t+1}| \leq Np_t$ **do**
  $\omega \leftarrow 0$
  $fixed_{new} \leftarrow [\,]$
  while $fixed_{new}$ *is empty* **do**
    Increase the order $\omega \leftarrow \omega + 1$
    List the cluster centres in $\widetilde{C}^{\omega}$ with smallest distances to each $w_i \in W_{free}^{t+1}$
    Set the cluster centre with the most weights assigned as $c_*^{\omega}(i)$
    Sort the weights $w_i \in W_{free}^{t+1}$ by their distance to $c_*^{\omega}(i)$
    do
      Append to $fixed_{new}$ the $w_i \in W_{free}^{t+1}$ with next smallest distance
    while *The mean* $D_{rel}^{+}(w \in fixed_{new}, c_*^{\omega}(i)) \leq \delta$
  Fix the all the weights in $fixed_{new}$ to cluster centre $c_*^{\omega}(i)$

A.2 DETAILS OF THE POWERS-OF-TWO APPROXIMATION ALGORITHM

We map our proposal set C^S to a ω-order approximation where each of the clusters $c_k \in C^S$ are written as ω powers-of-two (Eq 8). We do so using Algorithm 2. Figure 5 demonstrates how the values of C^S are rounded given different orders.

$$c_k = \sum_{j=1}^{\omega} r_j,\ r_j \in \{-\frac{1}{2^b}, \ldots, -\frac{1}{2^{j+1}}, -\frac{1}{2^j}, 0, \frac{1}{2^j}, \frac{1}{2^{j+1}}, \ldots \frac{1}{2^b}\} \tag{8}$$

Algorithm 2: Determining possible clusters

Input: The full precision proposal set: C^S, allowable relative distance: δ, pow2 rounding function: $round(x) = sgn(x)2^{\lfloor log_2(x) \rceil}$
Output: An order ω precision cluster set: $\widetilde{C}^{\omega}$
$\widetilde{C}^{\omega} \leftarrow [\,]$
for $c_k \in C^S$ **do**
  $c'_k = round(c_k)$
  for $i = 0 \rightarrow \omega$ **do**
    $\delta_{c_k} \leftarrow c_k - c'_k$
    if $|\delta_{c_k}| \geq \delta c_k$ **then**
      $c'_k \leftarrow c'_k + round(\delta_{c_k})$
    end
  end
  $\widetilde{C}^{\omega} \leftarrow \widetilde{C}^{\omega} \cup \{c'_k\}$
end

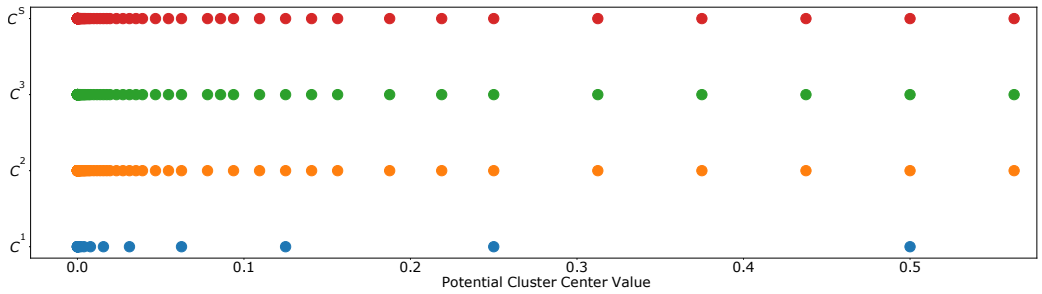

Figure 5: Approximating clusters in C^S with different orders

A.3 Reducing δ

To account for the observation that smaller relative distances are well tolerated in the early stages but less so as the final weights are quantised (high t), δ linearly. For any given $t \in T$ we use $\delta^t = \delta(T - t + 1)$ as our threshold.

A.4 Experiment Details

We give a full breakdown of the parameters used across all experiments ran in Table 3.

Model	Data	Opt	LR	T	Epochs per T	Batch size	γ	α
ResNet-18	ImageNet	Adam	2e-4	10	3	128	{0.05, 0.025, , 0.015, 0.01, 0.0075, 0.005}	{0.2, 0.4}
ResNet-34	ImageNet	Adam	2e-4	10	3	64	{0.05, 0.025, , 0.015, 0.01, 0.0075, 0.005}	{0.4}
ResNet-50	ImageNet	Adam	2e-4	10	3	64	{0.05, 0.025, , 0.015, 0.01, 0.0075, 0.005}	{0.4}
GoogLeNet	ImageNet	Adam	2e-4	10	3	64	{0.01, 0.0075, 0.015}	{0.4}
ResNet-18	CIFAR-10	Adam	3e-4	10	{3, 5, 10}	512	{0.01, 0.02, 0.03, 0.04, 0.05}	{0.0, 0.1, 0.2, 0.4, 0.8}
MobileNet	CIFAR-10	Adam	2e-4	10	{3, 5, 10}	512	{0.01, 0.02, 0.03, 0.04, 0.05}	{0.0, 0.1, 0.2, 0.4, 0.8}

Table 3: Full set of hyper-parameters explored for each model-dataset combination.

A.5 Hyper-parameter Exploration

We conducted a hyper-parameter search on both the ResNet-18 and MobileNet (Figures 6, 7). We find similar results across models when selecting hyper-parameters, and additionally, we observe that as we increase the regularisation term weighting, a weight-space entropy reduction. Further, we found that negating this term altogether $\alpha = 0$ has the surprising effect of increasing the resultant entropy values and causes an accuracy performance drop, demonstrating the utility of the regularisation term.

A.6 Layerwise Breakdown

In Figure 8 we examine how the parameter count and layer-parameter entropy change with each layer for both the WFN and APoT approaches. We find both gains over the unquantised layers of APoT, but also that the entropy and parameter count in the convolutional layers (those quantised by APoT) are similar.

A.7 A Full Metric Comparison

In Table 4 we give the full metric breakdown comparing WFN to the state-of-the-art APoT work. We calculate the unique parameter count and entropy values for subsets of the weights. No BN corresponds to all weights other than those in the batch-norm layers, and No BN-FL is the set of weights not including the first-last and batch-norm layers. It's clear here that WFN outperforms APoT even when we discount the advantage gained of taking on the challenge of quantising all layers.

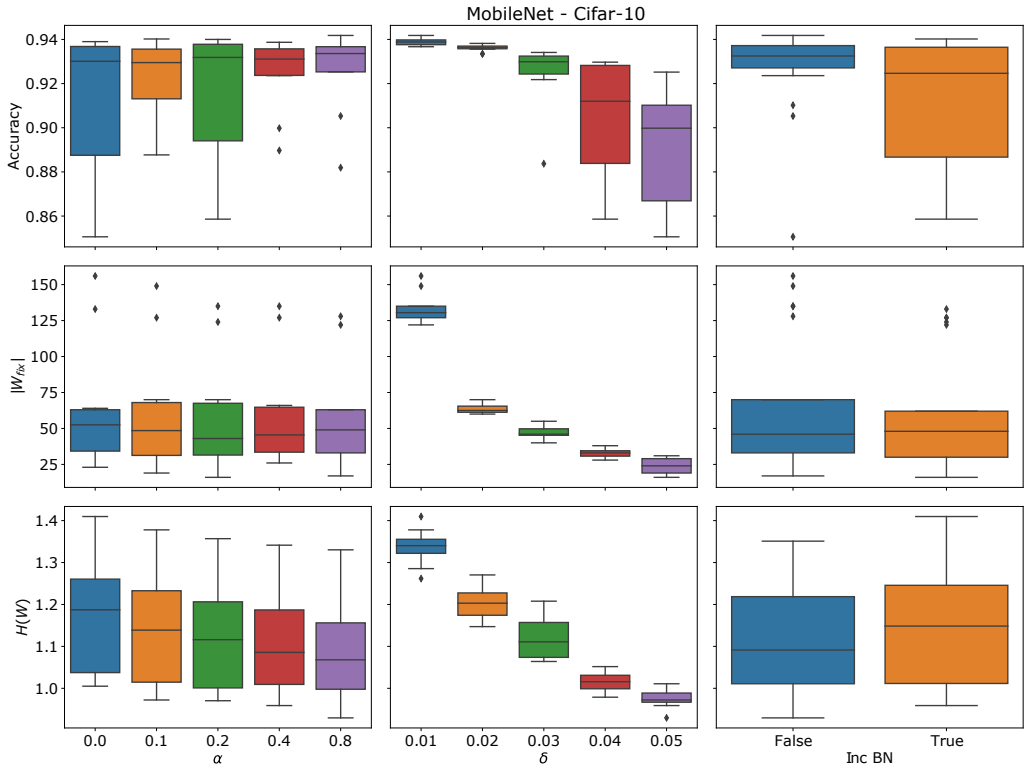

Figure 6: Experiments exploring the hyper-parameter space with MobileNet model trained on the CIFAR-10 dataset. Columns; **Left:** varying the regularisation ratio α, middle: varying the distance change value δ, **Right:** whether we fix the batch-norm variables. Rows; top: top-1 accuracy test-set CIFAR-10, **Middle:** total number of network weights, bottom: entropy of the weights.

			Full Network		No BN		No BN-FL		
Model	**Method**	**Top-1**	**Entropy**	**Param Count**	**Entropy**	**Param Count**	**Entropy**	**Param Count**	**Model Size**
ResNet-18	Baseline	68.9	23.3	10756029	23.3	10748288	23.3	10276369	46.8MB
	APoT (3bit)	69.9	5.77	9237	5.76	1430	5.47	274	4.56MB
	WFN ($\delta = 0.015$)	67.3	2.72	90	2.71	81	2.5	81	3.5MB
	WFN ($\delta = 0.01$)	69.7	3.01	164	3.00	153	2.75	142	3.8MB
	WFN ($\delta = 0.0075$)	70.3	4.15	193	4.13	176	3.98	162	4.6MB
ResNet-34	Baseline	73.3	24.1	19014310	24.1	18999320	24.10	18551634	87.4MB
	APoT (3bit)	73.4	6.77	16748	6.75	16474	6.62	389	8.23MB
	WFN ($\delta = 0.015$)	72.2	2.83	117	2.81	100	2.68	100	6.9MB
	WFN ($\delta = 0.01$)	72.6	3.48	164	3.47	132	3.35	130	7.9MB
	WFN ($\delta = 0.0075$)	73.0	3.87	233	3.85	191	3.74	187	8.5MB
ResNet-50	Baseline	76.1	24.2	19915744	24.2	19872598	24.20	18255490	97.5MB
	WFN ($\delta = 0.015$)	75.1	3.55	125	3.50	105	3.42	102	9.3MB
	WFN ($\delta = 0.01$)	75.4	4.00	199	3.97	169	3.88	163	10.0MB
	WFN ($\delta = 0.0075$)	76.0	4.11	261	4.09	223	4.00	217	10.2MB

Table 4: A full metric comparison of WFN Vs. APoT. We compare the unique parameter count and entropy of all parameters in the full network, as well as the same measures but not including the batch-norm layers (No BN) and the parameters not including the batch-norm and first and last layers (No BN-FL).

A.8 Pruning Experiments

To explore how WFN interacts with pruning we conduct a simple set of experiments. Instead of starting the WFN process with all weights un-fixed we randomly select $p\%$ of the weights to be pruned in each layer. We then run WFN as before starting with $p_t = p$, reducing the number of T iterations. The results, shown in Figure 9, are conducted with a ResNet-18 and Cifar-10 combination, painting a mixed picture. On the one hand, WFN and pruning at lower levels ($< 50\%$) is well tolerated and provide two benefits, a lower weight-space entropy and few weight-fixing iterations. On the other hand, full-precision networks can tolerate much higher ranges of pruning so there it would seem that a certain amount of synergy between the two approaches is present but this

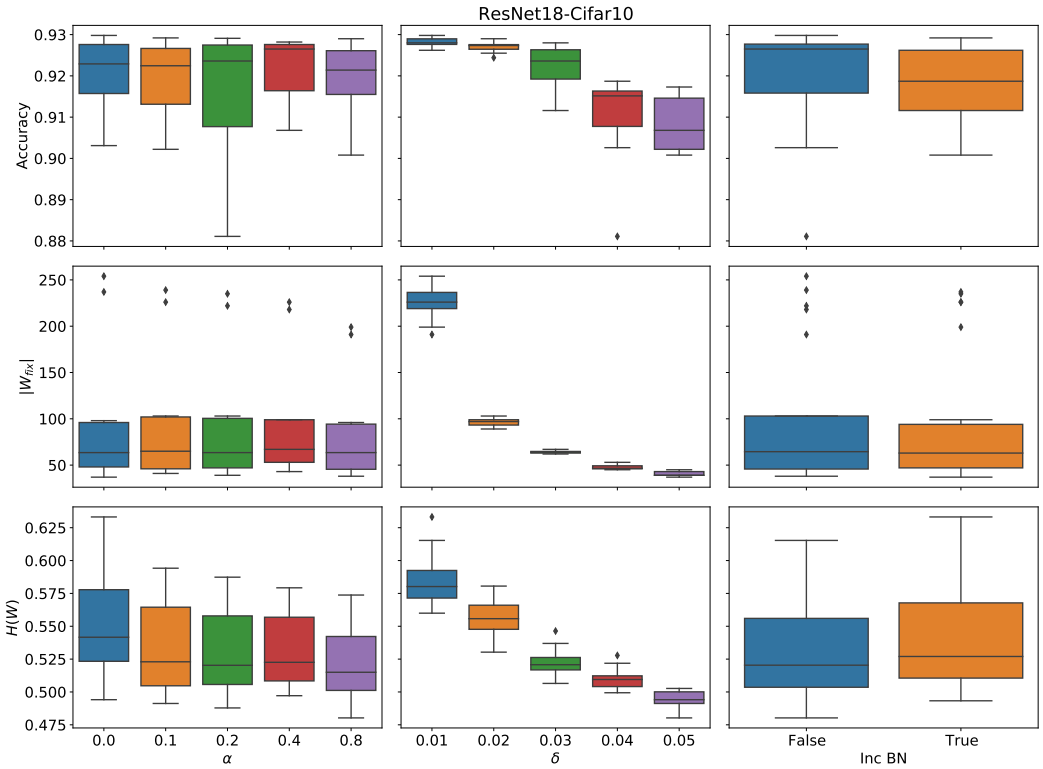

Figure 7: Experiments exploring the hyper-parameter space with ResNet18 model trained on the CIFAR-10 dataset. Columns; **Left:** varying the regularisation ratio α, **Middle:** varying the distance change value δ, **Right:** whether we fix the batch-norm variables. Rows; **Top:** top-1 accuracy test-set CIFAR-10, middle: total number of network weights, bottom: entropy of the weights.

is tempered compared to full precision networks.

It's important to note that WFN already has a form of pruning built-in with the δ_0 value balancing the emphasis on pruning over quantisation.

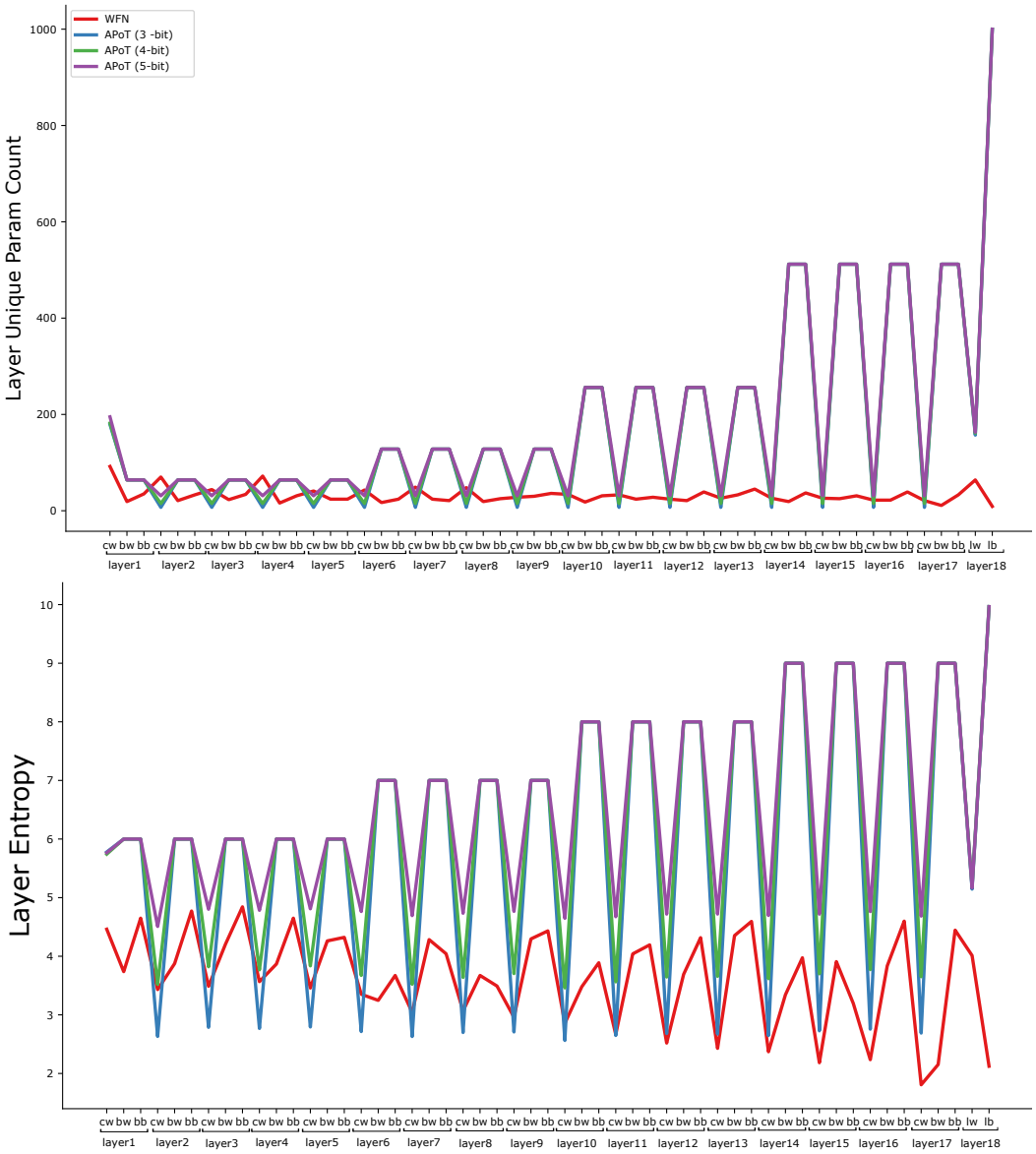

Figure 8: We compare WFN with a traditional quantisation set-up (APoT) with varying bit-widths applied to a ResNet18 model trained on the ImageNet dataset. The top chart shows the layerwise unique parameter count where WFN has consistently fewer unique parameters per layer.

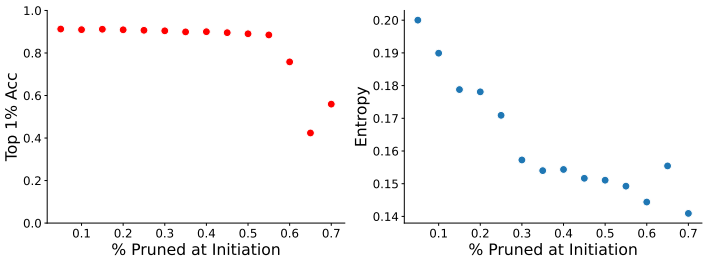

Figure 9: How does WFN and random pruning at initialisation interact?